SUPERHYDROPHOBIC STAINLESS STEEL SURFACE BY TWO-STEP NS LASER PROCESSING

PETR HAUSCHWITZ[1,2*], RADKA BICISTOVA[1], JAGDHEESH RADHAKRISHNAN[1], JAN BRAJER[1], DANIJELA ROSTOHAR[1]

[1]Hilase Centre, Institute of Physics, Academy of Sciences of the Czech Republic, Dolni Brezany, Czech Republic.
[2]Faculty of Nuclear Sciences and Physical Engineering, Czech Technical University in Prague, Prague, Czech Republic
DOI: 10.17973/MMSJ.2019_12_2019116
e-mail: petr.hauschwitz@hilase.cz

Growing demand for superhydrophobic surfaces in recent years is associated to many attractive science and engineering applications including self-cleaning, anti-icing and anti-corrosive behaviours. Stainless steel type AISI 316L is one of the most versatile and widely used engineering material in industries. Inspired by the "lotus effect" nano/microstructures has been fabricated by direct laser writing method with nanosecond laser source using two ablation regimes. Primarily, microstructures were fabricated with a tightly focused beam and covered by nano-scale structures by defocused laser beam in the second fabrication step. However, freshly prepared laser patterned metal surface shows hydrophilic behaviour. The hydrophilic to superhydrophobic transformation takes several days or weeks by aging technique in atmospheric condition. In this study, the transition time has been drastically reduced by high vacuum processing technique. Wetting properties with respect to laser processing parameters and surface morphology were examined and found to be consistent for large droplet volumes.

KEYWORDS

Laser micromachining, superhydrophobicity, functional surfaces, stainless steel.

1 INTRODUCTION

Fabrication of superhydrophobic surfaces draw a lot of attention in recent years due to many potential applications in science and industry including production of anti-corrosion [Khorsand et al. 2016], anti-bacteria [Zhao et al. 2018], anti-icing [Bharathidasan et al. 2014] or self-cleaning surfaces [Bhushan et al. 2009].

Inspired by the nature, many fabrication methods have been developed to replicate extremely water repellent lotus leave surface covered with hierarchical dual-scale micro and nanostructures [Liu et al. 2010] including lithography [Shiu et al. 2004], chemical etching [Cremaldi et al. 2018], chemical vapor deposition [Kamal et al. 2015], electrodeposition [Liu et al. 2016], sol-gel [Lakshmi et al. 2009] , thermal embossing [Toosi et al. 2016], and laser surface texturing [Jagdheesh et al. 2019].

Among these techniques, laser surface texturing offers flexible, non-contact method for fast and efficient nano and microstructure fabrication over large areas without need of additional chemical treatment. Moreover, the fabrication speed can be scaled up several times using polygonal scanners [De Loor 2013], multi-beam and interference processing [Aguilar-Morales et al. 2018] reaching 0.9 m^2/min [Lang et al. 2016].

However, metal oxide layer formed after laser processing on the top of the geometries results in a hydrophilic nature of processed sample. Exposed to atmospheric conditions, several days to a few weeks are required for transition from hydrophilic to hydrophobic or superhydrophobic state [Kietzig et al. 2009]. This time can be dramatically reduced to a several hours by vacuum processing introduced by Jagdheesh [Jagdheesh et al. 2017].

Wettability of a rough surface can be described by two well-know theories. According to Wenzel model [Wenzel 1936] for a fully-wetted rough surface, an originally hydrophilic surface (contact angle (CA) < 90°) becomes more hydrophilic with increased roughness and hydrophobic surface (CA > 90°) properties are also enhanced with increased roughness. Contrarily, Cassie-Baxter model [Cassie et al. 1944] describing the surface able to keep air pockets inside surface features shows improvement of hydrophobic character with increasing roughness even for originally hydrophilic flat samples.

In this paper, a nanosecond laser source is used to produce a combination of micro and nanostructures in a two-step fabrication process on AISI 316L steel, which is commonly used in industrial contexts such as medical implants, precision mechanics, marine applications and food handling. In the first step microstructures are made by a tightly focused beam and covered by nanoscale-protrusions in the second step using defocused laser beam. Wettability of textured surfaces is analyzed with respect to geometry and processing parameters.

2 MATERIAL AND METHODS

AISI 316L stainless steel plates were used as received (Ra ~ 0.3 µm) and treated in air with nanosecond Ytterbium fiber laser with a wavelength of 1062 nm and output power of 12 W, pulse duration of 3 ns and adjustable repetition rate in a rage of 100-1000 kHz. Galvanometric scanner system with 163 mm F-theta lens was used for beam displacement over the sample with the maximum available scanning speed of 700 mm/s.

Sample was processed in two steps in order to fabricate hierarchical dual-scale structures. In the first step, a tightly focused beam with 39 µm in diameter was used to produce micropillars by moving the laser beam in a rectangular grid path with a hatch distance (HD) in a rage of 30 – 50 µm and with up to 400 overscans. Laser repetition rate and pulse energy were optimized during the process for best quality micropillars. In the second step, beam was defocused by moving the sample closer to the laser source by a defocusing distance (*d*) and scanned line by line over the whole sample with a line hatch distance of 0,5 µm and single overscan, which results in a formation of nanoscale features on the top of micropillars as it was demonstrated in our previous work [Hauschwitz et al. 2019].

Samples were put into vacuum chamber immediately after laser treatment and kept in high vacuum ($2.6 \cdot 10^{-6}$ Pa) for 12 hours to promote favourable chemical changes to decrease transition time between hydrophilic and hydrophobic state.

Surface morphology were examined with a laser confocal microscope Olympus OLS5000. Wettability of laser-treated samples were measured with optical contact angle measuring device OCA 15EC, Data Physics Instruments using 10 µl droplets of deionized water. The results were acquired through the average of 5 measurements on different locations for every sample surface.

3 RESULTS AND DISCUSSION

Thermal processes including rapid heating and boiling of the melt are connected with nanosecond ablation [Leitz et al. 2011], resulting in the melt ejection and forming of a recast layer around the interaction zone. Therefore, laser and processing parameters have to be properly optimized to ablate well-defined structures with minimal unwanted thermal effects.

Tightly focused beam with a train of nanosecond pulses is used in the first fabrication step with the aim to produce high quality and melt-free micropillars with a maximum possible depth. The quality of produced micropillars was optimized by changing repetition rate, pulse energy and hatch distance, while keeping the power and scanning speed at the maximum level, as depicted in the Fig. 1. The micropillar height evolution in a dependence on repetition rate and pulse energy is shown in the Fig. 2.

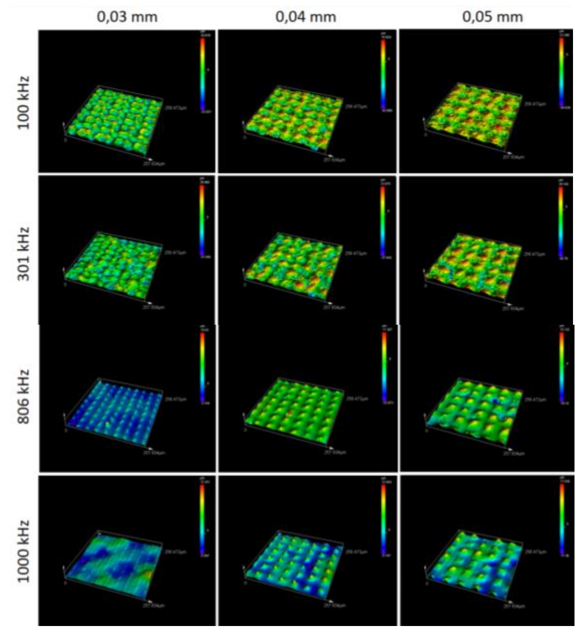

Figure 1. Representative confocal images of fabricated micropillars with the repetition rate in a rage of 100 kHz to 1 MHz and HD in a rage of 30 µm to 50 µm.

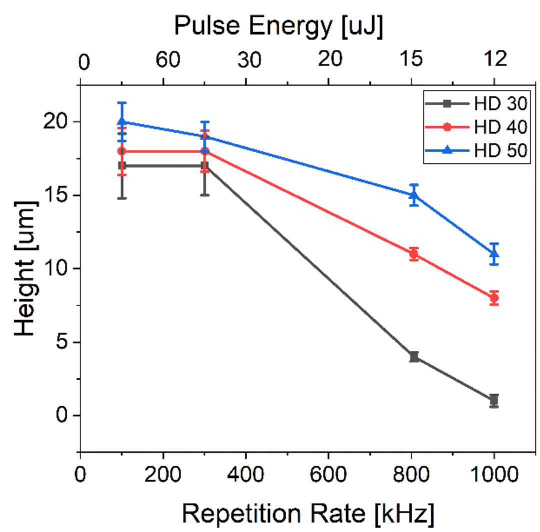

Figure 2. Micropillar height dependence on the repetition rate and pulse energy for 30 µm, 40 µm and 50 µm hatch distance.

As can be observed in Fig. 1, too small hatch distance, below 40 µm can result in an irradiation of the whole area leading to a smaller pillar high, especially when a high number of pulses is hitting the same spot due to high repetition rate > 800 kHz, as demonstrated in the Fig. 2. This behavior can be explained by the accumulation effect between consecutive laser pulses. Due to gaussian distribution of the laser beam, the edges of the beam are below ablation threshold. However, when high number of pulses are hitting the same spot due to high repetition rate, accumulation between consecutive laser pulses leads to temperature increase on the target between these pulses and results in a decrease in ablation threshold [Weber et al. 2014]. Therefore, a bigger part of a gaussian beam is above the threshold and material can be ablated in a wider area. As a result, width and depth of produced structures is reduced for high repetition rates, as depicted in Fig. 1. Contrarily, due to same pump power, pulse energy is decreasing with higher repetition rate decreasing the effective beam diameter. However, the accumulation effect is much more significant, as demonstrated in Fig. 1.

Therefore, the highest pillars were demonstrated for the lowest used repetition rate of 100 kHz with enough spacing between pillars (HD of 50 µm), as shown in Fig. 2. According to the analysis of suitable microstructure geometry for superhydrophobicity [Kong et al. 2019], the micropillar height is an important aspect which should generally improve water repellency when increased. Hence, surface with the highest micropillars (Figure 3) was selected as the optimal surface for the further fabrication step.

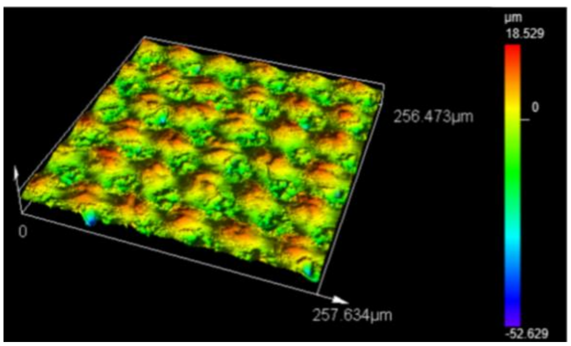

Figure 3. Confocal image of the optimal surface topography after the first fabrication step with 100 kHz repetition rate and 50 µm hatch distance, 400 overscans.

In the second step, defocused laser beam is introduced on the surface with previously fabricated micropillars in order to produce nanoscale features on the top of them by gently melting the surface without removing the structures. For this purpose, hatch distance was decreased to 0.5 µm to introduce high enough line to line overlap for melting the surface with defocused beam. Repetition rate and defocusing distance had to be further optimized to prevent overwriting microstructures from the first fabrication step, as depicted in Fig. 4. Power and scanning speed were kept at maximum for higher processing rates.

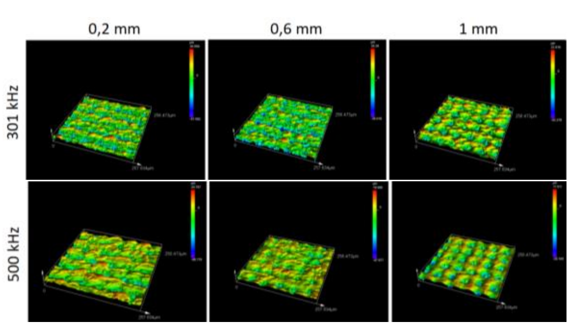

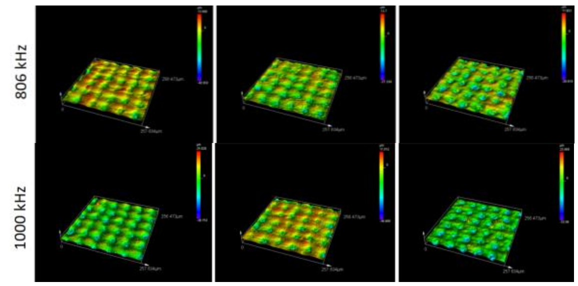

Figure 4. Representative confocal images of structure evolution for repetition rate in a range of 300 – 1000 kHz and defocusing distance in a range of 0.2 – 1 mm, during second fabrication step.

Higher pulse energy (RR < 500 kHz) and short defocusing distance (d < 0.6 mm) results in high intensity on a surface and removal of micropillars from the surface, as can be observed in the Fig. 4. By decreasing repetition rate or increasing defocusing distance above these values, gently melted micropillar surface, covered with nanoscale features can be fabricated. Contrarily, too small intensity (RR > 1 MHz, d > 1 mm) only heats up the surface without melting and no nanostructures are formed (results not shown). Optimal surface after second fabrication step is depicted in Figure 5.

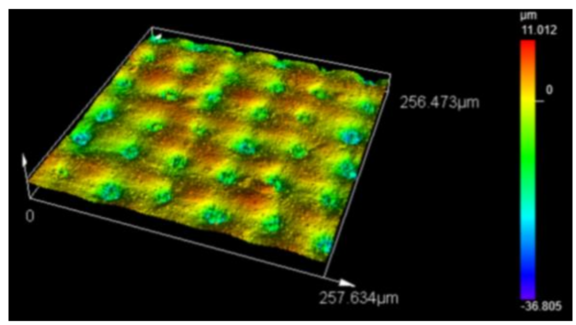

Figure 5. Confocal image of the optimal surface example after second fabrication step. Sample was fabricated with 1 MHz repetition rate, 0.6 mm defocusing distance and single overscan.

All samples are superhydrophilic after processing due to formation of metaloxydes with high surface energy. It takes a few days to few weeks for samples kept in an atmospheric conditions to reach superhydrophobic properties [Kietzig, Hatzikiriakos and Englezos 2009]. Therefore, immediately after laser processing samples were put in a vacuum chamber and kept in the high vacuum conditions ($2.6 \cdot 10^{-6}$ Pa) for 12 hours**.** This vacuum processing technique introduced by Jagdheesh [Jagdheesh, Diaz, Marimuthu and Ocana 2017] significantly reduces the time needed for wettability transition from hydrophilic to superhydrophobic state by preventing water molecules to form a passivation layer which slows down the evolution of non-polar hydrocarbon layer primarily responsible for superhydrophobic behaviour.

After vacuum processing, wettability of selected best quality hierarchical structures was analysed with 10 µl droplets of deionized water and sessile drop technique. These results are depicted in the Fig. 6.

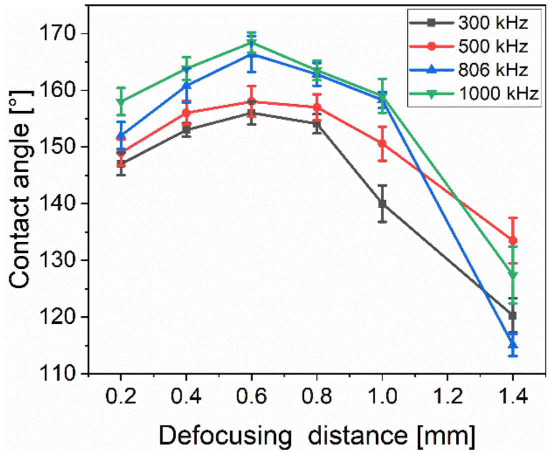

Figure 6. Contact angle evolution with the defocusing distance for different repetition rates.

Contact angles were measured only for defocusing distances above 0.4 mm. Below this value, most of the micropillars were removed during the second fabrication step. As depicted in Fig. 6, there is an optimal defocusing distance around 0.6 mm when contact angle reaches its maximum for all used repetition rates. A sharp decrease in contact angle is observed for defocusing distance above 0.8 mm. It can be explained by the drop in intensity on the surface which is not high enough for creation of nano-scale features. The highest contact angle of 168° was reached for the surface fabricated with 1 MHz and 0.6 mm defocusing distance. Droplet deposited on this surface can be observed in Fig. 7. The detail look on the contact area reveals that droplet is deposited only on the top of produced micropillars and it is not wetting the whole surface. Therefore, surface is in a Cassie-Baxter state.

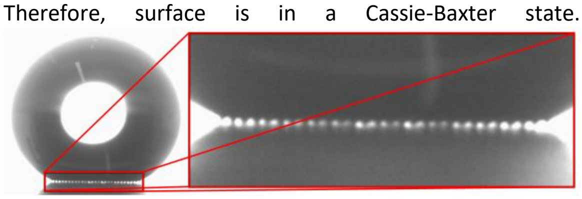

Figure 7. Detail of a droplet deposited on an extremely water repellent surface fabricated with 1 MHz and 0.6 mm defocusing distance in a second fabrication step.

4 CONCLUSION

Well-defined micro pillars covered with nanoscale protrusions were fabricated with properly optimized nanosecond laser source using the two-step fabrication technique. The height and width of micropillars can be controlled by repetition rate and hatch distance during the first fabrication step. In the second step, nanoscale protrusions are fabricated on the top of micropillars without removing the original structure, when defocusing distance and repetition rate are properly optimized. The wettability transition time from freshly processed hydrophilic sample to superhydrophobic was significantly reduced by vacuum processing technique. The best wettability result with contact angle of 168° was reached for surface produced with 100 kHz and 50 µm hatch distance in the first step, followed by the second processing step with 1 MHz and 0.5 µm hatch distance, defocused for 0.6 mm above the surface.

Acknowledgements

Funding: This work was supported by European Structural and Investing Funds, Operational Programme Research, Development and Education (Grant agreement NO CZ.02.1.01/0.0/0.0/15_006/ 0000674) and from the European Union's Horizon 2020 research and innovation programme (Grant agreement NO 739573), and by the Ministry of Education, Youth and Sports of the Czech Republic (Programmes NPU I-Project no. LO1602 and Large Research Infrastructure Project No. LM2015086).

REFERENCES

[Aguilar-Morales 2018] AGUILAR-MORALES, A. I., et al. Micro-fabrication of high aspect ratio periodic structures on stainless steel by picosecond direct laser interference patterning. Journal of materials processing technology, February 2018, Vol. 252, pp 313-321. ISSN 0924-0136

[Bharathidasan 2014] BHARATHIDASAN, T., et al. Effect of wettability and surface roughness on ice-adhesion strength of hydrophilic, hydrophobic and superhydrophobic surfaces. Applied surface science, September 2014, Vol. 314, pp 241-250. ISSN 0169-4332

[Bhushan 2009] BHUSHAN, B., et al. Micro-, nano-and hierarchical structures for superhydrophobicity, self-cleaning and low adhesion. Philosophical Transactions of the Royal Society A: Mathematical, Physical and Engineering Sciences, May 2009, Vol.367, No.1894., pp 1631-1672. ISSN 1364-503X

[Cassie 1944] CASSIE, A., et al. Wettability of porous surfaces. Transactions of the Faraday society, June 1944, Vol.40, ISSN 546-551.

[Cremaldi 2018] CREMALDI, J., et al. Fabrication of bioinspired, self-cleaning superliquiphilic/phobic stainless steel using different pathways. Journal of colloid and interface science, May 2018, Vol.518, pp 284-297. ISSN 0021-9797

[De Loor 2013] DE LOOR, R. Polygon scanner system for ultra short pulsed laser micro-machining applications. Physics Procedia, 2013, Vol.41, pp 544-551. ISSN 1875-3892

[Hauschwitz 2019] HAUSCHWITZ, P., et al. Nanostructure fabrication on the top of laser-made micropillars for enhancement of water repellence of aluminium alloy. Materials Letters, December 2019, Vol.256, ISSN 0167-577X

[Jagdheesh 2017] JAGDHEESH, R., et al. Robust fabrication of µ-patterns with tunable and durable wetting properties: hydrophilic to ultrahydrophobic via a vacuum process. Journal of Materials Chemistry A, March 2017, Vol.5, No.15., ISSN 7125-7136.

[Jagdheesh 2019] JAGDHEESH, R., et al. Non-fluorinated superhydrophobic Al7075 aerospace alloy by ps laser processing. Applied surface science, November 2019, Vol. 493, pp 287-293. ISSN 0169-4332

[Kamal 2015] KAMAL, S. A. A., et al. Wetting behaviour of carbon nitride nanostructures grown by plasma enhanced chemical vapour deposition technique. Applied surface science, February 2015, Vol.328, pp 146-153. ISSN 0169-4332

[Khorsand 2016] KHORSAND, S., et al. Corrosion behaviour of super-hydrophobic electrodeposited nickel–cobalt alloy film. Applied surface science, February 2016, Vol.364, pp 349-357. ISSN 0169-4332

[Kietzig 2009] KIETZIG, A.-M., et al. Patterned superhydrophobic metallic surfaces. Langmuir, March 2009, Vol.25, No.8., pp 4821-4827. ISSN 0743-7463

[Kong 2019] KONG, T., et al. Bioinspired Superwettability Micro/Nanoarchitectures: Fabrications and Applications. Advanced Functional Materials, January 2019, Vol.29, No.11., ISSN 1616-301X

[Lakshmi 2009] LAKSHMI, R., et al. Fabrication of superhydrophobic sol–gel composite films using hydrophobically modified colloidal zinc hydroxide. Journal of colloid and interface science, November 2009, Vol.339, No.2., pp 454-460. ISSN 0021-9797

[Lang 2016] LANG, V., et al. World record in high speed laser surface microstructuring of polymer and steel using direct laser interference patterning. Laser-Based Micro- and Nanoprocessing X: 16-18 February 2016, San Francisco, California, ISBN 978-1-628-41971-9

[Leitz, et al. 2011] LEITZ, K.-H., et al. Metal ablation with short and ultrashort laser pulses. Physics Procedia, 2011, Vol.12, pp 230-238. ISSN 1875-3892

[Liu 2010] LIU, K., et al. Recent developments in bio-inspired special wettability. Chemical Society Reviews, December 2010, Vol.39, No.8., pp 3240-3255. ISSN 3240-3255.

[Liu 2016] LIU, Y., et al. Superhydrophobic and superoleophobic surface by electrodeposition on magnesium alloy substrate: wettability and corrosion inhibition. Journal of colloid and interface science, September 2016, Vol.478, pp 164-171. ISSN 0021-9797

[Shiu 2004] SHIU, J.-Y., et al. Fabrication of tunable superhydrophobic surfaces by nanosphere lithography. Chemistry of materials, January 2004, Vol.16, No.4., pp 561-564. ISSN 0897-4756

[Toosi 2016] TOOSI, S. F., et al. Microfabrication of polymeric surfaces with extreme wettability using hot embossing. Applied surface science, August 2016, Vol.378, pp 426-434. ISSN 0169-4332

[Weber 2014] WEBER, R., et al. Heat accumulation during pulsed laser materials processing. Optics express, 2014, Vol.22, No.9., pp 11312-11324. ISSN 1094-4087

[Wenzel 1936] WENZEL, R. N. Resistance of solid surfaces to wetting by water. Industrial & Engineering Chemistry, August 1936, Vol.28, No.8., pp 988-994. ISSN 0019-7866

[Zhao 2018] ZHAO, Y., et al. Corrosion resistance and antibacterial properties of polysiloxane modified layer-by-layer assembled self-healing coating on magnesium alloy. Journal of colloid and interface science, April 2018, Vol.526, pp 43-50. ISSN 0021-9797

CONTACTS

Petr Hauschwitz
Hilase Centre, Institute of Physics, Academy of Sciences of the Czech Republic, Za Radnici 828, Dolni Brezany 25241, Czech Republic
petr.hauschwitz@hilase.cz